Journal of Magnetic Resonance 329 (2021) 107030

Contents lists available at ScienceDirect

Journal of Magnetic Resonance

journal homepage: www.elsevier.com/locate/jmr

Quantification of magic angle spinning dynamic nuclear polarization NMR spectra

Andrea Bertarello [a], Pierrick Berruyer [a], Urban Skantze [b], Samiksha Sardana [c], Malvika Sardana [c], Charles S. Elmore [c], Markus Schade [d], Elisabetta Chiarparin [d], Staffan Schantz [e], Lyndon Emsley [a,*]

[a] Institut des Sciences et Ingénierie Chimiques, École Polytechnique Fédérale de Lausanne, Lausanne, Switzerland
[b] Advanced Drug Delivery, Pharmaceutical Science, AstraZeneca, Gothenburg, Sweden
[c] Early Chemical Development, Pharmaceutical Science, R&D, AstraZeneca, Gothenburg, Sweden
[d] Chemistry, Oncology R&D, AstraZeneca, Cambridge, United Kingdom
[e] Oral Product Development, Pharmaceutical Technology & Development, Operations, AstraZeneca, Gothenburg, Sweden

ARTICLE INFO

Article history:
Received 3 May 2021
Revised 22 June 2021
Accepted 25 June 2021
Available online 28 June 2021

Keywords:
Dynamic nuclear polarization
Quantification
Magic angle spinning

ABSTRACT

Dynamic nuclear polarization (DNP) allows to dramatically enhance the sensitivity of magic angle spinning nuclear magnetic resonance (MAS NMR). DNP experiments usually rely on the detection of low-γ nuclei hyperpolarized from ^{1}H with the use of cross polarization (CP), which assures more efficient signal enhancement. However, CP is usually not quantitative. Here we determine the quantification performance of three different approaches used in MAS NMR, (conventional CP, variable contact time CP, and multiple-contact CP) under DNP conditions, and we show that absolute quantification in MAS DNP NMR is possible, with errors below 10%.

1. Introduction

Solution-state nuclear magnetic resonance (NMR) is a potent tool for quantification [1]. Since the first quantitative applications in the 1960s [2–3], NMR has been extensively used to accurately quantify analytes in a large variety of systems.

However, despite its extremely high versatility, NMR suffers from inherently low sensitivity, especially when compared to other analytical techniques used for quantification, such as mass-spectrometry [4–6], even if improvements in NMR technology have allowed to significantly lower the limit of detection and quantification in solution NMR [7]. Moreover, the applicability of solution NMR to quantification is biased to the study of molecules in the fast motional regime, and large molecules or molecules in rigid or highly viscous matrixes often escape detection.

Magic Angle Spinning (MAS) NMR allows the analysis of immobilized molecules, with virtually no limit regarding size [8–9]. The sensitivity of MAS NMR can be dramatically increased with the use of Dynamic Nuclear Polarization (DNP), through the transfer of electron spin polarization from a paramagnetic agent to nearby nuclear spins upon irradiation with microwaves (μw) [10–11].

DNP experiments usually rely on the observation of low-γ nuclei, such as ^{13}C. Due to long polarization build up times, direct excitation of ^{13}C is usually not performed. Moreover, with DNP, direct excitation of ^{13}C does not provide quantitative spectra due to the lack of efficient spin diffusion to distribute the hyperpolarization [12–13]. Alternatively, ^{13}C spins can be hyperpolarized from ^{1}H using cross polarization (CP), with simultaneous radio-frequency irradiation on ^{1}H and ^{13}C [14]. The typically faster DNP build-up times of ^{1}H hyperpolarization usually result in more efficient signal enhancement. However, ordinary CP is usually not quantitative, mostly due to the fact that magnetization transfer from ^{1}H to directly bonded ^{13}C is faster compared to quaternary ^{13}C or more mobile portions of the molecule [15].

Different approaches have been proposed in MAS NMR in order to make conventional CP at the Hartmann-Hahn condition [16] more quantitative. These include the use of ramped CP [17], ^{13}C–^{13}C spin diffusion [18,19], variable contact time CP [20,21], multi-pulse irradiation [22], and multiple-contact CP [23,24]. Multiple-contact CP, in particular, has already proven to be effective in providing reliable relative quantification in polymers under DNP conditions [13]. In another application, multiple-contact CP has also been shown to efficiently transfer surface-based hyperpolarization into the bulk of inorganic solids [25,26].

Here, we develop a CP based absolute quantification approach using an internal standard for MAS DNP NMR. We explore the

* Corresponding author.
E-mail address: lyndon.emsley@epfl.ch (L. Emsley).

https://doi.org/10.1016/j.jmr.2021.107030
1090-7807/

quantification performance of three different approaches used in MAS NMR, notably conventional CP, variable contact time CP, and multiple-contact CP, under DNP conditions. The experiments are performed on benchmark frozen solutions, each containing a standard and an analyte in known amounts, and on a more complex mixture where signal overlap occurs. The analytes range from simple metabolites such as sodium pyruvate, to a medium sized drug molecule. We show that absolute quantification in MAS DNP NMR is possible, with errors below 10%. All of the aforementioned experimental approaches provide reliable quantification, to some degree, but we find that multiple-contact CP clearly provides the best results in terms of robustness, reproducibility, efficiency and accuracy.

2. Experimental

2.1. Sample preparation

Six samples (numbered 1 to 6) are analyzed here, as summarized in Fig. 1. Samples 1 to 4 are prepared by mixing a standard and an analyte in a known amount of D_2O (Sigma-Aldrich), as described below.

The amount of analyte is verified by solution NMR. Each solution is then mixed with suitable amounts of H_2O, $^{12}C_3$, $^2H_8$ - glycerol (Cambridge Isotope Laboratories), and AMUPol [27] (kindly provided by Dr O. Ouari), in order to obtain a preparation corresponding to glycerol:D_2O:H_2O 6:3:$1_{v/v}$ AMUPol 10 mM [27,28].

Sample 1 was obtained by mixing 37.7 mg of calcium formate as a standard (Sigma-Aldrich, TraceCERT®) with 28.4 mg of imidazole·HI as an analyte (TCI), in 1114.7 mg of D_2O.

Sample 2 was obtained by mixing 14.3 mg of calcium formate as a standard (Sigma-Aldrich, TraceCERT®) with 0.7 mg of $^{13}C_6$ - Wnt-c59 as an analyte (provided by AstraZeneca), in 2 mL of D_2O (volumetric flask).

Sample 3 is obtained by mixing 36.0 mg of imidazole·HI as a standard (TCI) with 0.7 mg of 1-^{13}C sodium pyruvate as an analyte (Camdridge Isotope Laboratories), in 1096.3 mg of D_2O.

Sample 4 was prepared from the same batch as *Sample 1*, but then analyzed as a repeat sample for DNP.

Sample 5 and *sample 6* were prepared from a mixture obtained by mixing 33.6 mg of a liposome suspension (~95 mg·mL^{-1} DPPC: DPPS 98:$2_{w/w}$ in D_2O, provided by AstraZeneca) with 60 μL of a $^2H_6$-DMSO:D_2O:H_2O 6:3:1v/v, 14 mM AMUPol solution ($^2H_6$-DMSO purchased from Cambridge Isotope Laboratories). This solution was split in two aliquots, one of which (*sample 5*) was added to 20 μL of the solution used to prepare sample 1 (calcium formate : imidazole in D_2O), while the other (sample 6) is used as a blank. Further details are provided in SI.

Solution NMR. ^{1}H 1D solution NMR experiments were acquired on a 400 MHz (9.4 T) Avance Neo Bruker NMR spectrometer equipped with a TBO 5 mm probe. The residual water signal is suppressed. For quantification, the recycle delay and the acquisition duration were set to 60 s and 5 s, respectively.

DNP MAS NMR. DNP enhanced solid-state NMR experiments for samples 1 to 3 were performed on a 400 MHz (9.4 T) Avance Neo III Bruker NMR spectrometer, coupled with a 263 GHz gyrotron microwave source and equipped with a 3.2 mm triple resonance low-temperature MAS probe tuned to ^{1}H, ^{13}C, ^{15}N. Experiments for samples 4 to 6 were performed on a 401 MHz (9.4 T) Avance Neo III Bruker NMR spectrometer, coupled with a 264 GHz klystron microwave source and equipped with a 3.2 mm triple resonance low-temperature MAS probe tuned to ^{1}H, ^{13}C, ^{15}N. Experiments were performed at ~ 100 K and at 8 kHz MAS (samples 1–4), and 7 kHz MAS (samples 5 and 6). For all cross polarization experiments the ^{1}H rf field was ramped from 90 to 100 % during the contact time. The recycle delay was set to 1.3 times the ^{1}H build up time, $T_{B,on}$. For variable contact time CP, the experiments were acquired by varying the contact time while keeping all the other experimental parameters unchanged. Multiple-contact CP experiments were acquired using the pulse scheme shown in Fig. 3**A** [25], with a recycle delay of 0.1 s, with variable number of CP loops (L) and durations of the inter-CP delay (τ_z), while all the other parameters are kept the same as in the other CP experiments. For samples 3 to 5 a single rotor period synchronized spin-echo is added prior to detection in order to minimize baseline distortions. Further details are provided in SI.

Quantification. The quantification for solution NMR, single CP and multiple-contact CP experiments is performed through the integrals of the ^{1}H (for solution NMR experiments) or ^{13}C (for MAS DNP NMR experiments) signals of interest using the following expression [29]:

$$m_x = \frac{I_x}{I_s} \cdot \frac{N_s}{N_x} \cdot \frac{M_x}{M_s} \cdot P_s \cdot m_s$$

where the subscripts x and *s* refer to the analyte and the standard, respectively. *m* is the mass of the sample, *I* is the NMR integral, *N* is the number of nuclei associated to a given signal, and *M* is the molar mass. P_s is a factor which takes into account the purity of the standard, and, for samples 2 and 3, also the natural abundance of ^{13}C (assumed here to be 1.07%) [30] for the cases where the analytes were ^{13}C-labeled but not the standards.

The mass determined with solution NMR is an average value from the signals shown in Figures S1 to S3. For sample 1 (and therefore sample 4) the value is an average over three different spectra, while for sample 3 the value is an average over two different spectra.

For variable contact time CP (VCP) the integrals of interest are plotted as a function of the contact time (for example as shown in Fig. 2). The quantification is performed using the intercepts

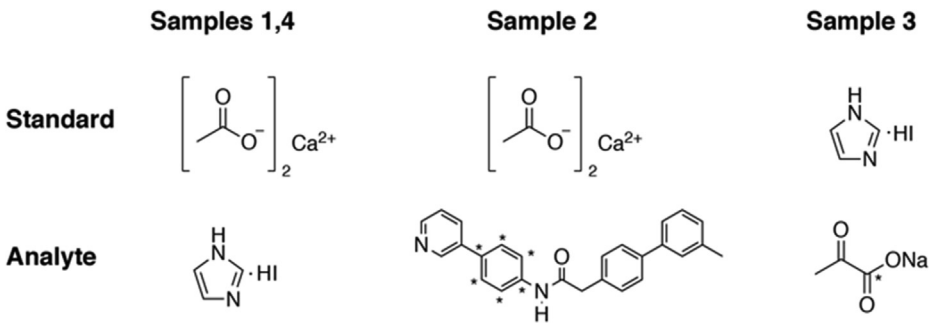

Fig. 1. Standards and analytes used for preparing samples 1 to 4. Samples 1 and 4 are prepared from the same starting stock solution, and then separately diluted to obtain the solutions for DNP. * indicates ^{13}C labeled atoms.

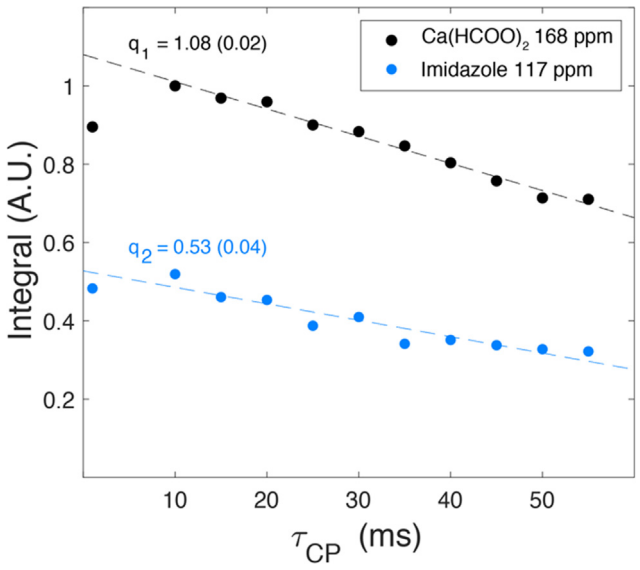

Fig. 2. VCP plot for sample 1. The black and cyan dots indicate the integrals for the calcium formate and the $C_{4,5}$ imidazole resonances, respectively. The lines indicate the linear regression, and q the intercepts with their respective error (the 95% confidence interval). The points at 1 ms are excluded from the fit. (For interpretation of the references to colour in this figure legend, the reader is referred to the web version of this article.)

obtained from the linear fitting of the data according to the following expression:

$$m_x = \frac{q_x}{q_s} \cdot \frac{N_s}{N_x} \cdot \frac{M_x}{M_s} \cdot P_s \cdot m_s$$

where q refers to the intercept value, and the other parameters are previously defined. Points corresponding to CP contact times shorter than 10 ms are excluded from the fit.

For sample 5, the quantification is performed after a subtraction procedure, as described in the SI.

Quantification errors in DNP MAS NMR (e_{qDNP}) are obtained from the masses of analyte determined in the DNP experiment ($m_{x,DNP}$) and in solution NMR ($m_{x,sol}$) in the following way:

$$e_{qDNP} = \frac{m_{x,DNP} - m_{x,sol}}{m_{x,sol}} \cdot 100\%$$

and the uncertainty (u) of the errors are estimated in the following way:

$$u = \frac{m_{x,DNP}}{m_{x,sol}} \cdot \left(\frac{\Delta m_{x,sol}}{m_{x,sol}} \cdot \frac{\Delta m_{x,DNP}}{m_{x,DNP}} \right)$$

where $\Delta m_{x,sol}$ represents the 95% confidence interval of the analyte mass as determined from solution NMR, while $\Delta m_{x,DNP}$ is defined for CP and multiple-contact CP as:

$$\Delta m_{x,DNP} = m_{x,DNP} \cdot \left(\frac{1}{SN_s} + \frac{1}{SN_x} \right)$$

where SN_s and SN_x represent the signal to noise ratios of the standard and the analyte signal, respectively, while for VCP $\Delta m_{x,DNP}$ is defined as

$$\Delta m_{x,DNP} = m_{x,DNP} \cdot \left(\frac{\Delta q_s}{q_s} \cdot \frac{\Delta q_x}{q_x} \right)$$

where Δq_s and Δq_x represent the 95% confidence interval of the intercept values. Further details are provided in the SI.

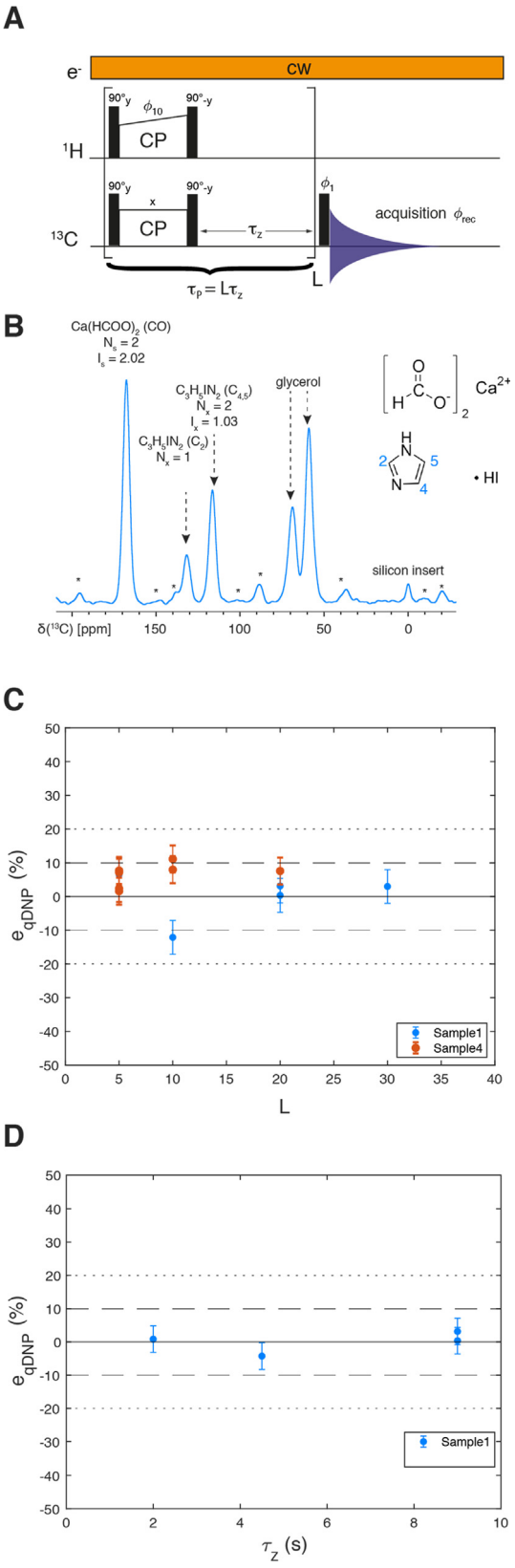

Fig. 3. (A) Multiple-contact DNP enhanced CP pulse scheme. (B) Multiple-contact DNP enhanced CP spectrum of sample 1 acquired at 9.4 T, 8 kHz MAS, ~100 K, with L = 5 and $\tau_z = 2*T_{B,on} = 9$ s (with a gyrotron μw source). N denotes the number of nuclei associated with a given signal, while I is the corresponding integral. (C, D) e_{qDNP} of the multiple-contact CP experiment for samples 1 and 4 as a function of L (C), and τ_z (D).

Table 1
e_{qDNP} (as defined in the experimental section) from DNP CP MAS experiments for samples 1 to 4 for single CP experiments shown for different CP contact times. An estimation of the uncertainty in the determined errors is provided in brackets for the points at τ_{CP} = 10 ms. *For sample 4 the values are the averages over two different measurements. More data points obtained from the variable contact time CP measurements, are provided in SI (Tables S1, S3-S5).

τ_{CP} (ms)	Sample 1	Sample 2	Sample 3	Sample 4*
10	+4 (5) %	−32 (16) %	+32 (12) %	+6 (5) %
20	−5%	−17%	+51%	−3%
30	−7%	−25%	+77%	−8%
40	−12%	−4%	+68%	−3%

Table 3
e_{qDNP} (as defined in the experimental section) for sample 1 as a function of L and τ_z ($T_{B,on}$ = 4.5 s). An estimation of the uncertainty of the determined errors for L = 5 is also provided.

L	τ_z (s)	Error
5	9	+3 (3)%
5	9	+7 (7)%
10	9	−12%
20	2	+1%
20	4.5	−4%
20	9	0%
20	9	+1%
30	9	+3%

3. Results and discussion

3.1. ***Samples and general*** *comments*

Fig. 1 shows the composition of the samples used here for quantification. All the samples are prepared from D_2O solutions of the standards and analytes, whose concentrations are verified by solution NMR. The frozen solutions are then analyzed in glycerol:D_2O:H_2O 6:3:$1_{v/v}$ AMUPol 10 mM [27–28] for the DNP experiments. The standards were chosen for the simplicity of their ^{1}H and ^{13}C spectra, and the absence of overlap with the NMR signals of interest in the analyte. Moreover, calcium formate is an established standard for quantitative solution NMR [31]. Wnt-c59 is an inhibitor of the PORCN pathway in human cells [32], and is representative of compounds of pharmacological relevance. The quantification is performed as described in the Experimental Section and in the SI.

Cross Polarization. Table 1 reports e_{qDNP}, relative to the amount of analyte determined with solution NMR, for samples 1 to 4, using ramped CP with different contact times. The errors range from 5 to 77%, and it can be seen that CP provides quantification accurate to less than 10% only for samples 1 and 4 (which are repeats with the same composition). The performance is worse for sample 2, and is completely unreliable for sample 3, for all the contact times used. Therefore, not unexpectedly, a simple CP experiment should not be considered generally applicable for quantification purposes in DNP MAS NMR.

Variable contact time CP. In variable contact time CP (VCP), a series of CP experiments with increasing contact times are acquired. The integrals of the signals of interest are plotted as a function of the contact time, and the quantification is performed from the extrapolation of the integrals to zero contact time [19–21]. An example is shown in Fig. 2 for sample 1. Typically points corresponding to CP contact times shorter than 10 ms are excluded from the fit since they are not yet in the linear regime. e_{qDNP} for samples 1 to 4 is reported in Table 2, together with the number points used for the fitting. The results show that VCP, similarly to single CP, does not provide reliable quantification for all the samples studied, and moreover that the quantification is subject to a large uncertainty. The performance is only slightly affected by the number of points used for the linear regression, as shown in the case of sample 1. The lower number of points recorded might partially explain the large error observed for samples 2 and 3, but also sets a limit on the applicability of the approach in the case of very dilute samples, where the simultaneous need for good signal to noise ratios from longer experiments and a sufficiently high number of points might lead to prohibitively long experimental times.

Multiple-Contact Cross Polarization. In multiple- contact cross polarization (Fig. 3**A**) the CP step is repeated several (L) times, interleaved with delays (τ_z) during which the ^{13}C magnetization is stored along the z-axis, and during which the ^{1}H magnetization recovers to a near-equilibrium value [24,25]. Multiple CP has already been shown to provide robust quantification in conventional MAS NMR, where integral peak intensities of ^{13}C signals usually show deviations not larger than 5% from the expected values after few CP cycles [24]. Moreover, the sequence is quite robust with respect to the choice of the different experimental parameters [24]. Besides the calibration of the ^{1}H and ^{13}C pulses, and the optimization of the CP conditions as in standard CP experiments, the sequence only requires the choice of the τ_z period, which should be on the order of $2{\cdot}T_{1,H}$, and the number of loops, L, which should be chosen large enough in order to provide effective saturation of the transferred polarization during $L{\cdot}\tau_z$. It should also be pointed out that, as already discussed [24], the CP contact time should be adapted to the $T_{1\rho,H}$ of the different species, in order to avoid any extensive differential relaxation of the signals which might reduce the quantification performance of multiple CP. Fig. 3**B** shows the ^{13}C multiple CP spectrum for sample 1, for L = 5 and $\tau_z = 2{\cdot}T_{B,on}$, where $T_{B,on}$ here refers to the ^{1}H DNP build-up time. Table 3 shows the quantification performance of the multiple CP experiment for sample 1 as a function of different values of L and τ_z. It is evident that, with the exception of two points, in all the other cases the sequence provides a robust quantification performance, with errors comprised between ± 5%, good reproducibility, and relatively low uncertainty. These results are also summarized in Fig. 3**-C-D**. Note that in Fig. 3**C** data for sample 4 are also reported. From the analysis of these data is evident that, in order for multiple-contact CP to provide reliable quantification, values of L = 5 and $\tau_z = 2{\cdot}T_{B,on}$ are sufficient in the test samples. Table 4 shows the

Table 4
e_{qDNP} (as defined in the experimental section) for samples 1 to 4 as obtained with multiple-contact CP, for L = 5 and $\tau_z = 2{\cdot}T_{B,on}$. An estimation of the uncertainty is also provided. *For samples 1 the value is the average over two different measurements. **For sample 4 the value is the average over four different measurements.

Sample 1	Sample 2	Sample 3	Sample 4
+5 (5) %	−6 (11) %	−7 (17) %	+5 (4) %

Table 2
e_{qDNP} (as defined in the experimental section) for samples 1 to 4 as obtained with variable contact time CP (number of points in brackets). An estimation of the uncertainty of the determined errors is also provided.

Sample 1 (11 points)	Sample 1 (4 points)	Sample 2 (4 points)	Sample 3 (5 points)	Sample 4 (12 points)
−1 (10) %	+4 (14) %	−32 (35) %	+35 (56) %	−1 (38) %

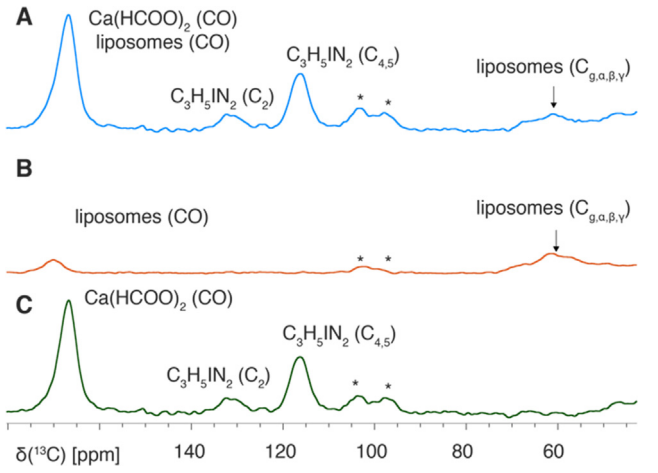

Fig. 4. Portion of the DNP enhanced multiple-contact CP spectrum of sample 5 (A) and sample 6 (B), acquired at 9.4 T, 8 kHz MAS, ~100 K, with L = 5 and $\tau_z = 2{\cdot}T_{B,on}$ = 11.5 s and a klystron μw source. (C) Spectrum used for quantification and obtained by subtracting (B) from (A), normalized by the liposomes signal marked with the arrow.

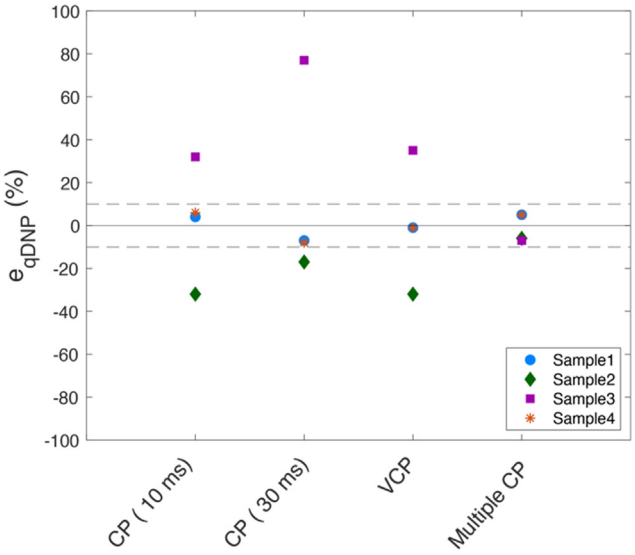

Fig. 5. Summary of the quantification performance in DNP enhanced MAS NMR for conventional CP (with 10 and 30 ms contact time), variable contact time CP, and multiple-contact CP (with L = 5 and $\tau_z = 2{\cdot}T_{B,on}$), for samples 1 to 4.

e_{qDNP} obtained for all the four samples, using L = 5 and $\tau_z = 2{\cdot}T_{B,on}$. Multiple-contact CP appears to perform considerably better than standard CP and VCP for all the four samples, with uncertainties consistently lower than those estimated for VCP, and comparable to those estimated for CP. Note also that for samples 1 and 4, which share the same composition, the same quantification performance is observed, supporting the reproducibility of the multiple-contact CP approach.

Table 4 summarizes the performance of multiple-contact CP for all four samples, and we again see that accurate quantification is obtained in all four sample, with errors less than 7%.

Mixtures. The multiple-contact CP approach is also tested in a more complex system, made up of a mixture of calcium formate and imidazole together with a preparation of DPPC/DPPS 98:$2_{w/w}$ liposomes (sample 5), in a ~ 2:1:0.2:0.01 molar ratio between calcium formate, imidazole, DPPC and DPPS. In the DNP enhanced multiple-contact CP spectrum of sample 5 (shown in Fig. 4**A**) the signal of calcium formate at ~ 170 ppm overlaps with signals arising from the liposome background, disabling the possibility of quantification. In order to remove the signal arising from the background, the DNP enhanced multiple-contact CP spectrum of the liposomes alone was acquired under the same conditions (sample 6, shown in Fig. 4**B**) and is subtracted from the spectrum of sample 5 by normalizing the intensity of both spectra to the signal at ~ 60 ppm (marked by an arrow in A-B), which arises only from the C_g, C_α, C_β, C_γ resonances of the liposomes. The resulting spectrum (shown in Fig. 4**C**), which eliminates the liposomes background, allows the quantification of the imidazole content in the sample, using the calcium formate as a standard, with e_{qDNP} comprised between −2 and −6% (more details are provided in the SI).

4. Conclusion

We have investigated the possibility to perform quantitative MAS DNP NMR using an internal standard. Three different approaches, namely CP, variable contact time CP, and multiple-contact CP, have been tested on simple mixtures containing a standard and an analyte in known amounts, in glycerol/DMSO water solutions and using AMUPol as the polarizing agent. In analogy to results from conventional solid-state NMR [24], as well as the performance in other DNP enhanced applications [13,26], multiple-contact CP is found to provide the best performance for quantitative DNP, with absolute errors in quantification usually less than 10%, and, as summarized in Fig. 5 for the cases here, appears to be the most robust, reproducible, efficient and accurate approach even in complex mixtures. While here we have analyzed relatively simple systems characterized by uniform enhancements between the analyte and the standard, we speculate that the quantification approach will be still applicable in more complex samples characterized by non-uniform enhancements, by dividing the corresponding integrals by their steady-state enhancements. We are currently investigating this aspect further. We would also like to mention that, as already extensively discussed [24], $T_{1,H}$, $T_{1,C}$, and $T_{1\rho,H}$ times of the analyzed species are critical factors, and the experimental parameters must be chosen accordingly for accurate quantification. In the case of very different relaxation times between the standard and the analyte the quantification might be less accurate or even rendered impractical (e.g. for $T_{1\rho,H}$ values when one of the signals of interest is a methyl group, or if there are specific interactions with the paramagnetic polarization source used for DNP).

We suggest that this simple and rapid high-sensitivity approach will provide a reliable tool for quantification of analytes in MAS DNP NMR.

Funding sources

This work was funded by the Swiss National Centre of Competence in Research (NCCR) Chemical Biology and AstraZeneca.

Declaration of Competing Interest

The authors declare that they have no known competing financial interests or personal relationships that could have appeared to influence the work reported in this paper.

Acknowledgment

We thank Dr. Snaedis Björgvinsdóttir (EPFL) for help implementing the multiple CP experiments and Dr. Olivier Ouari (Aix Marseille Univ) for providing the AMUPol radical.

Appendix A. Supplementary material

Supplementary data to this article can be found online at https://doi.org/10.1016/j.jmr.2021.107030.

References

[1] S.K. Bharti, R. Roy, Quantitative 1H NMR spectroscopy, TrAC, Trends Anal. Chem. 35 (2012) 5–26.
[2] D.P. Hollis, Quantitative Analysis of Aspirin, Phenacetin, and Caffeine Mixtures by Nuclear Magnetic Resonance Spectrometry, Anal. Chem. 35 (11) (1963) 1682–1684.
[3] J.L. Jungnickel, J.W. Forbes, Quantitative Measurement of Hydrogen Types by Intergrated Nuclear Magnetic Resonance Intensities, Anal. Chem. 35 (8) (1963) 938–942.
[4] R. Khatun, H. Hunter, W. Magcalas, Y. Sheng, B. Carpick, M. Kirkitadze, Nuclear Magnetic Resonance (NMR) Study for the Detection and Quantitation of Cholesterol in HSV529 Therapeutic Vaccine Candidate, Comput. Struct. Biotechnol. J. 15 (2017) 14–20.
[5] T.E. Angel, U.K. Aryal, S.M. Hengel, E.S. Baker, R.T. Kelly, E.W. Robinson, R.D. Smith, Mass spectrometry-based proteomics: existing capabilities and future directions, Chem. Soc. Rev. 41 (10) (2012) 3912–3928.
[6] A.-H. Emwas, R. Roy, R.T. McKay, L. Tenori, E. Saccenti, G.A.N. Gowda, D. Raftery, F. Alahmari, L. Jaremko, M. Jaremko, D.S. Wishart, NMR Spectroscopy for Metabolomics Research. *Metabolites* 9 (7) (2019) 123.
[7] U. Holzgrabe, Quantitative NMR spectroscopy in pharmaceutical applications, Prog. Nucl. Magn. Reson. Spectrosc. 57 (2) (2010) 229–240.
[8] T. Polenova, R. Gupta, A. Goldbourt, Magic Angle Spinning NMR Spectroscopy: A Versatile Technique for Structural and Dynamic Analysis of Solid-Phase Systems, Anal. Chem. 87 (11) (2015) 5458–5469.
[9] Reif, B.; Ashbrook, S. E.; Emsley, L.; Hong, M., Solid-state NMR spectroscopy. Nature Reviews Methods Primers: in press.
[10] Q.Z. Ni, E. Daviso, T.V. Can, E. Markhasin, S.K. Jawla, T.M. Swager, R.J. Temkin, J. Herzfeld, R.G. Griffin, High Frequency Dynamic Nuclear Polarization, Acc. Chem. Res. 46 (9) (2013) 1933–1941.
[11] A.J. Rossini, A. Zagdoun, M. Lelli, A. Lesage, C. Copéret, L. Emsley, Dynamic Nuclear Polarization Surface Enhanced NMR Spectroscopy, Acc. Chem. Res. 46 (9) (2013) 1942–1951.
[12] T. Maly, A.-F. Miller, R.G. Griffin, In situ High-Field Dynamic Nuclear Polarization—Direct and Indirect Polarization of 13C nuclei, ChemPhysChem 11 (5) (2010) 999–1001.
[13] N.J. Brownbill, R.S. Sprick, B. Bonillo, S. Pawsey, F. Aussenac, A.J. Fielding, A.I. Cooper, F. Blanc, Structural Elucidation of Amorphous Photocatalytic Polymers from Dynamic Nuclear Polarization Enhanced Solid State NMR, Macromolecules 51 (8) (2018) 3088–3096.
[14] A. Pines, M.G. Gibby, J.S. Waugh, Proton-enhanced NMR of dilute spins in solids, J. Chem. Phys. 59 (2) (1973) 569–590.
[15] L.B. Alemany, D.M. Grant, R.J. Pugmire, T.D. Alger, K.W. Zilm, Cross polarization and magic angle sample spinning NMR spectra of model organic compounds. 1. Highly protonated molecules, J. Am. Chem. Soc. 105 (8) (1983) 2133–2141.
[16] S.R. Hartmann, E.L. Hahn, Nuclear Double Resonance in the Rotating Frame, Phys. Rev. 128 (5) (1962) 2042–2053.
[17] G. Metz, M. Ziliox, S.O. Smith, Towards quantitative CP-MAS NMR, Solid State Nucl. Magn. Reson. 7 (3) (1996) 155–160.
[18] G. Hou, F. Deng, S. Ding, R. Fu, J. Yang, C. Ye, Quantitative cross-polarization NMR spectroscopy in uniformly 13C-labeled solids, Chem. Phys. Lett. 421 (4) (2006) 356–360.
[19] K. Takeda, Y. Noda, K. Takegoshi, O. Lafon, J. Trébosc, J.-P. Amoureux, Quantitative cross-polarization at magic-angle spinning frequency of about 20kHz, J. Magn. Reson. 214 (2012) 340–345.
[20] M.S. Solum, R.J. Pugmire, D.M. Grant, Carbon-13 solid-state NMR of Argonne-premium coals, Energy Fuels 3 (2) (1989) 187–193.
[21] L.M. McDowell, A. Schmidt, E.R. Cohen, D.R. Studelska, J. Schaefer, Structural Constraints on the Ternary Complex of 5-Enolpyruvylshikimate-3-phosphate Synthase from Rotational-echo Double-resonance NMR, J. Mol. Biol. 256 (1) (1996) 160–171.
[22] L. Quiroga, J. Virlet, NMR cross polarization in solids using multipulse irradiation, J. Chem. Phys. 81 (11) (1984) 4774–4781.
[23] S. Zhang, X. Wu, M. Mehring, Successive polarization under mismatched Hartmann—Hahn condition, Chem. Phys. Lett. 166 (1) (1990) 92–94.
[24] R.L. Johnson, K. Schmidt-Rohr, Quantitative solid-state 13C NMR with signal enhancement by multiple cross polarization, J. Magn. Reson. 239 (2014) 44–49.
[25] S. Björgvinsdóttir, B.J. Walder, A.C. Pinon, L. Emsley, Bulk Nuclear Hyperpolarization of Inorganic Solids by Relay from the Surface, J. Am. Chem. Soc. 140 (25) (2018) 7946–7951.
[26] S. Björgvinsdóttir, B.J. Walder, N. Matthey, L. Emsley, Maximizing nuclear hyperpolarization in pulse cooling under MAS, J. Magn. Reson. 300 (2019) 142–148.
[27] C. Sauvée, M. Rosay, G. Casano, F. Aussenac, R.T. Weber, O. Ouari, P. Tordo, Highly Efficient, Water-Soluble Polarizing Agents for Dynamic Nuclear Polarization at High Frequency, Angew. Chem. Int. Ed. 52 (41) (2013) 10858–10861.
[28] G.J. Gerfen, L.R. Becerra, D.A. Hall, R.G. Griffin, R.J. Temkin, D.J. Singel, High frequency (140 GHz) dynamic nuclear polarization: Polarization transfer to a solute in frozen aqueous solution, J. Chem. Phys. 102 (24) (1995) 9494–9497.
[29] F. Malz, H. Jancke, Validation of quantitative NMR, J. Pharm. Biomed. Anal. 38 (5) (2005) 813–823.
[30] F.S. Midani, M.L. Wynn, S. Schnell, The importance of accurately correcting for the natural abundance of stable isotopes, Anal. Biochem. 520 (2017) 27–43.
[31] M. Weber, C. Hellriegel, A. Rueck, J. Wuethrich, P. Jenks, Using high-performance 1H NMR (HP-qNMR®) for the certification of organic reference materials under accreditation guidelines—Describing the overall process with focus on homogeneity and stability assessment, J. Pharm. Biomed. Anal. 93 (2014) 102–110.
[32] K.D. Proffitt, B. Madan, Z. Ke, V. Pendharkar, L. Ding, M.A. Lee, R.N. Hannoush, D.M. Virshup, Pharmacological Inhibition of the Wnt Acyltransferase PORCN Prevents Growth of WNT-Driven Mammary Cancer, Cancer Res. 73 (2) (2013) 502–507.